SPACE-VARIABLE FILTERING FOR APPROXIMATION OF UNIFORMLY SAMPLED IMAGES FROM SAMPLES ON IRREGULAR GRIDS

Ryszard Stasiński

Inst. of Electronics and Telecom.
Technical University of Poznań
Piotrowo 3A, PL-60-965 Poznań
Poland
`rstasins@et.put.poznan.pl`

Janusz Konrad

Dept. of Electrical and Computer Eng.
Boston University
8 Saint Mary's Street, Boston,
MA 02215, USA
`jkonrad@bu.edu`

ABSTRACT

The paper presents a space-variable POCS-based (projection onto convex sets) method for the reconstruction of a regularly-sampled image from its irregularly-spaced samples. Such reconstruction is often needed in image processing and coding, for example in stereo vision and motion compensation. The proposed approach applies two operators sequentially: bandwidth limitation and sample substitution, and is based on our earlier work. The contribution of this paper is the space-variable implementation of bandwidth limitation operator, which has been postulated previously. The operator is realized in the simplest possible way as a filter with two sets of coefficients, a measure of local density of irregular grid determines which set is used. The technique is efficient computationally although at the cost of increased memory requirements. Experimental results demonstrate that indeed, the new technique is much better in terms of PSNR, convergence speed, and visual quality than methods described previously.

1. INTRODUCTION

For working properly a typical display equipment for visualization of space-discrete signals requires that data to be presented are evenly distributed along display axes. Similarly, uniform sample distribution in space and/or time is a necessary condition for majority of digital signal processing methods and algorithms. On the other hand, a natural result of some advanced signal processing techniques is an irregularly sampled signal, e.g. A/D conversion at very high clock speeds, time- or space-variant filtering by stretching or contracting filter impulse responses, motion compensated frame interpolation in video, image interpolation in stereovision, some color coding techniques etc. At the same time simplistic approaches to interpolation of data on uniform sampling grids often give unacceptable results.

The emerging applications caused that high-quality methods for interpolation of evenly distributed samples from irregularly sampled signals have recently drawn attention of signal processing community [1, 2, 3, 4, 5]. However, as it is pointed out in [4], the methods does not adapt to local image properties, which result in trade-offs in image quality between regions that are 'easy' and 'difficult' to approximate. For example, the method from [4] is based on repetitive filtering of data; fine-tuned filters give better appearance to approximated images, however, they fail completely to reconstruct regions where sampling grid is too sparse. On the other hand, filters with greater attenuation of medium and high image frequencies, thus blurring somewhat images, work better in such image regions, which results even in higher PSNR values.

In this paper a high-quality method for interpolating of evenly distributed samples from irregularly sampled signals based on POCS approach that uses space variable filters is presented, section 2. Namely, one of two POCS steps, the repetitive image filtering is done by a FIR filter having two sets of coefficients, one for spectrum limitation at Nyquist frequency, and the other for a filter with approximately two times narrower bandwidth. A simple grid density function is introduced, its local value implies which set of filter coefficients is used for image filtering. As can be seen from Fig.2, section 3, the approach indeed improves convergence and final PSNR of the algorithm. The filter is working on 4 times denser sampling grid for approximating continuous-space image, relatively high memory cost of the method is its only drawback, if compared to that from [4]. Otherwise, the method is very simple, and relatively time-efficient.

2. METHOD

Let $g = \{g(\mathbf{x}), \mathbf{x} = (x, y)^T \in R^2\}$ be a continuous 2-D projection of the 3-D world onto an image plane and let $g_\Lambda = \{g(\mathbf{x}), \mathbf{x} \in \Lambda\}$ be a discrete image obtained

from g by sampling over a lattice Λ [6]. Let's assume that g is band-limited, i.e., $G(\mathbf{f}) = \mathcal{F}\{g\}=0$ for $\mathbf{f} \notin \Omega$ where $\mathcal{F}$ is the Fourier transform, $\mathbf{f} = (f_1, f_2)^T$ is a frequency vector and $\Omega \subset R^2$ is the spectral support of g. If the lattice Λ satisfies the multi-dimensional Nyquist criterion [6], the Shannon sampling theory allows to perfectly reconstruct g from g_Λ. However, in the case of irregular sampling the theory is not applicable. Therefore, the general goal is to develop a method for the reconstruction of g from an irregular set of samples $g_\Psi = \{g(\mathbf{x}_i), \mathbf{x}_i \in \Psi \subset R^2, i = 1, ..., K\}$, where Ψ is an irregular sampling grid.

2.1. POCS-based reconstruction algorithm

We use the POCS methodology [7] to reconstruct image g. This methodology involves a set theoretic formulation, i.e., finding a solution as an intersection of property sets rather than by a minimization of a cost function. We use the following sets [1, 4, 5, 8]:

- A_0 - set of all images g such that at $\mathbf{x}_i \in \Psi$, $i = 1, ..., K$ (irregular sampling grid) $g(\mathbf{x}_i) = g_\Psi(\mathbf{x}_i)$,

- A_1 - set of all band-limited images g, i.e., such that $G(\mathbf{f}) = 0$ for $\mathbf{f} \notin \Omega$.

If the membership in A_0 can be assured by a sample replacement operator $\mathcal{R}$ (to enforce proper image values on Ψ), and the membership in A_1 – by suitable bandwidth limitation (low-pass filtering) $\mathcal{B}$, then the iterative reconstruction algorithm can be expressed as follows [1]:

$$g^{k+1} = \mathcal{B}\mathcal{R}g^k = \mathcal{B}[g^k + \mathcal{S}_\Psi(g - g^k)], \quad (1)$$

where g^k is the reconstructed image after k iterations and $\mathcal{S}_\Psi$ is a sampling operator that extracts image values (luminance/color) on the irregular grid Ψ.

In order to implement equation (1) on a computer, a suitable discretization must to be applied. Since our goal is the reconstruction of image samples obtained from motion or disparity compensation, a 1/2-, 1/4- or 1/8-pixel precision of motion or disparity vectors is usually sufficient. Therefore, it has been proposed to implement (1) on an oversampled grid matching that precision [4, 5, 8]:

$$g^{k+1}_{\Lambda_P} = \mathcal{B}[g^k_{\Lambda_P} + \lambda \mathcal{S}_{\Psi/\Lambda_P}(g_{\Psi/\Lambda_P} - g^k_{\Lambda_P})]. \quad (2)$$

where $\mathcal{B}$ is implemented on Λ_P, that is a $P \times P$-times denser (oversampled) lattice than Λ, and P equals not more than 16 depending on motion/disparity vector precision. Clearly, Λ is a sub-grid of Λ_P, i.e., $\mathbf{x} \in \Lambda \Rightarrow \mathbf{x} \in \Lambda_P$. g_{Ψ/Λ_P} is the nearest-neighbor interpolation of g_Ψ on Λ_P, defined at each $\mathbf{x}_i \in \Psi$ as follows:

$$g_{\Psi/\Lambda_P}(\mathbf{y}) = \begin{cases} g_\Psi(\mathbf{x}_i) & \text{if } \|\mathbf{x}_i - \mathbf{y}\| \leq \|\mathbf{x}_i - \mathbf{z}\|, \\ 0 & \text{otherwise.} \end{cases} \quad (3)$$

for all $\mathbf{y}, \mathbf{z} \in \Lambda_P$. Similarly, $\mathcal{S}_{\Psi/\Lambda_P}$ denotes the nearest-neighbor sampling, i.e., sampling on $\mathbf{y} \in \Lambda_P$ that is nearest to $\mathbf{x}_i \in \Psi$. In other words, the implementation (2) is performed on a denser lattice Λ_P and the positions of the irregular samples from Ψ are quantized to the nearest position on Λ_P. This allows us to avoid the cumbersome interpolations done in [1] under the assumption that a suitable value of P is selected.

2.2. Adaptation of the relaxation coefficient

The choice of the relaxation coefficient λ in equation (2) has a direct impact on the convergence properties of the algorithm; the greater the λ, the faster the convergence, but only up to some λ_{max} above which the algorithm becomes unstable. Experiments have shown that the value of λ_{max} in (2) is closely related to the properties of the irregular sampling grid. Namely, the algorithm has been most prone to instability in image regions where irregular sampling grid is the densest. Clearly, when increasing λ above λ_{max}, the algorithm starts to diverge in those image regions where the number of irregular samples per area is the highest. That is why it is proposed to introduce an additional λ-correcting term in equation (2) as follows [4, 5]:

$$g^{k+1}_{\Lambda_P} = \mathcal{B}[g^k_{\Lambda_P} + (\lambda/d_\Psi)\mathcal{S}_{\Psi/\Lambda_P}(g_{\Psi/\Lambda_P} - g^k_{\Lambda_P})]. \quad (4)$$

where d_Ψ are samples of a function describing local density of irregular grid. The algorithm implementations based on (4) allow higher values of λ_{max}, and therefore faster convergence than those based on formulation (2). As it turns out, the values of λ_{max} become only marginally dependent on the degree of variation in the local densities of irregular grids.

To be a good descriptor of local grid density, the function d should equal 1 where the grid is regular, should be greater than 1 in areas where there are more samples of irregular grid than those of regular one, and no more than 1 when converse is true. Experiments show that the actual definition of the function is not critical; various functions d seem to work almost equally well.

2.3. Implementation

2.3.1. Lowpass filtering operator

Properties of the low-pass filter implementing the $\mathcal{B}$ operator in (4) are crucial for the algorithm's performance. Let's assume for now that the relaxation parameter λ equals 0. Then, the algorithm (4) degenerates to repetitive filtering of the initial data set. In frequency domain, such a repetitive filtering is equivalent to a repetitive multiplication by filter's frequency

response that results in increasing amplification of the signal for frequency bands where filter's magnitude response is greater than 1, and increasing attenuation where this response is less than 1. Non-ideal filter frequency response influences algorithm stability, therefore in [5] two constraints has been imposed on it. Firstly, the filter should be 'passive', i.e., its frequency response should satisfy:

$$|H(\omega)| \le 1, \forall \omega \qquad (5)$$

This requirement is particularly important for frequency $\omega = 0$ since images intensities are non-negative, and, moreover, have large DC component. Indeed, it has been observed that for filters that amplify image DC component, formula (4) is unstable.

Secondly, it is desirable that for passband frequencies, $|H(\omega)|$ be equal to 1.0, or very close to it. In such a situation, the relaxation coefficient λ in (4) need not compensate for the attenuation of past results. Once more, this is particularly important for the DC component of an image. Hence, the second constraint is:

$$|H(0)| = 1. \qquad (6)$$

This means that the frequency response of the filter has (local) maximum for $\omega = 0$.

At a glance, it seems that the amount of filter attenuation in the stopband is not critical, since the repetitive filtering enhances it quite effectively. Experiments show, however, that good attenuation is important for the removal of high-frequency components of recent corrections in (4). Clearly, it appears that for best results the error weights in passband and stopband in the Remez exchange algorithm for equiripple FIR filters should be approximately the same.

An important result of [4] is that generally very good filters fail to operate correctly in image areas where local density of irregular sampling grid is too low. The best space-invariant filter seems to be the compromise one, the overall sharp and contrasty interpolated image apperance is in contradiction with sizes and intensities of false black spots in ill-defined image regions. That is why the use of space-variable filters is analyzed in the paper.

2.3.2. Local grid density function

It has been observed in [4] that the actual definition of the local density grid function d_Ψ in (4) has little influence on the performance of the whole algorithm. This means that a simplified approach to its definition should work as well. Therefore, the function d_Ψ can be obtained by smoothing out (or spreading) the following 'presence' function (3):

$$\vartheta(\mathbf{x}) = sign\{g_{\Psi/\Lambda_P}(\mathbf{x})\}, \qquad \mathbf{x} = [x, y]^T$$

i.e., the function that is equal to 1 at nearest-neighbour positions from Ψ, and zero otherwise. The smoothing filter should have non-negative impulse response, as local density function cannot be negative, and should retain the signal energy. We are implementing two smoothing filters, one obtained from impulse response:

$$h_i(x) = [0.05, 0.17, 0.56, 0.17, 0.05],$$

described earlier in [4, 5] is used for computing d_Ψ in (4); the other one used for evaluating local grid density to control the space-variable bandwidth limiting operator is based on filter

$$h_f(x) = (25/17)[0.05, 0.17, 0.24, 0.17, 0.05].$$

The smoothing filters are defined as follows: $h(x) = P^2 h_1(x) * h_2(x) * ... * h_P(x)$, where $*$ is the convolution operator ($P - 1$ times self-convolution and suitable gain). This 1-D filter horizontal filter is convolved with its transposed (vertical) sibling to obtain a separable 2-D FIR filter. Both density grid functions, including d_Ψ, are therefore obtained by the following filtering:

$$d_\Psi(x, y) = \vartheta(x, y) * h(x) * h(y).$$

To avoid problems with divisions by zero in (4), all "unused" samples of the resultant density grid function d_Ψ in (4), i.e., not coinciding with positions in Ψ, have been set to 1.0.

3. EXPERIMENTAL RESULTS

The method has been implemented in *Matlab*, and tested on a pair of ITU-R 601-resolution stereoscopic images *Flowerpot*, Fig.3, in the context of disparity-compensated interpolation: the right image has been reconstructed by applying disparity field to the approximation of the left image. Namely, grid samples of the approximated left images have been obtained by reverse application of disparity field to the right image, and then by bicubic interpolation, which technique eliminates errors of disparity field [4].The algorithm has been tested for oversampling ratio $P = 4$.

The space-variable bandwidth limiting operator $\mathcal{B}$ (4) has been realized in the simplest possible way as a pair of separable low-pass FIR filters: basic one with passband around Nyquist frequency, and narrowband one, choice of filter for generating a pixel has been done on the basis of local grid density function value. The filters have been designed using the Remez exchange algorithm for linear-phase equiripple FIR filters with some modifications. Namely, although the method allows easy determination of band edges and ratio of ripples in the passband and stopband, there is no direct way to impose the constraint that filter frequency response have maximum at $\omega = 0$. However,
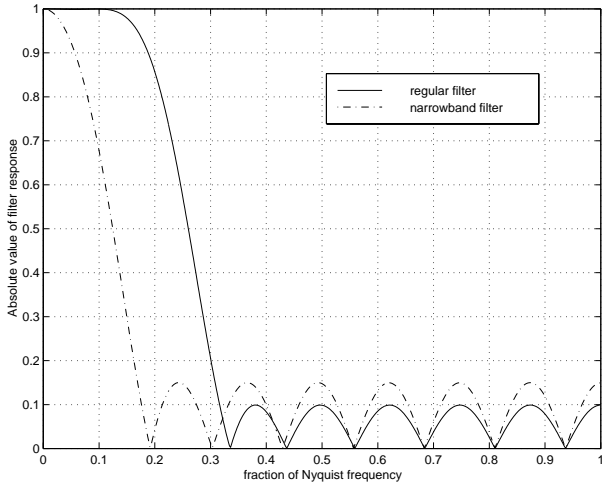
Figure 1: Frequency responses of filters used for construction of space variable bandwidth limiting operator $\mathcal{B}$ in (4).
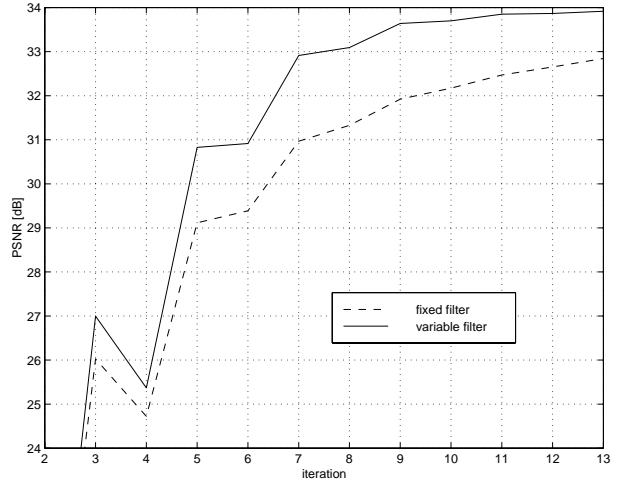

Figure 2: Evolution of the luminance reconstruction error of *Flowerpot* image interpolated using space-variable and fixed filters.

Figure 3: Original right image from the stereo pair *Flowerpot*.

this requirement has appeared to be crucial for the efficiency of the whole algorithm. The desired filter property has been obtained by splitting filter passband into two parts: one from frequency 0 to 0.01π, and the second from 0.02π to the required passband edge, frequency response in the second band has been described not as a flat one, but rising from some value $1 - \alpha$ to 1, α has been found experimentally. Additionally, error weights in filter bands have been set to 100 for the band from 0 to 0.01π, and to 1 for the remaining two bands, and band edges slightly modified. Relatively short 17-tap filters have been used, the transition band of the regular filter has been originally set to $0.75/P$ and $1.25/P$ of Nyquist frequency, i.e. from $(3/16)\pi$ to $(5/16)\pi$, compare [8, 4, 5]). It appeared that reasonable narrowband filter passband and transition band could not be narrower than approximately half of those for the regular filter, Fig.1. Then, filter coefficients have been normalized by dividing them by their sum, i.e., by $H(0)$. In this way, the conditions (5) and (6) have been met.

Results for the space-variable filter have been compared to those for a fixed filter, here they have been obtained using the same filter with the narrowband filtration switched off. Relaxation coefficient has been set to $\lambda = 0.7$, higher values are possible, but they result in stronger oscillations in PSNR curves. The treshold between regular and narrowband filtration has been set experimentally to 0.67, i.e. narrowband filtration is executed in regions where on the average they are less than approximately 2 irregular samples in the area associated with 3 regular grid positions (grid Λ). As can be seen from Fig.2, higher performance of space-variable filter in terms of PSNR and

convergence rate is evident.

What is even more important, the new realization of $\mathcal{B}$ operator (4) seems to solve problems with locally ill-defined sampling grids. In Fig.4 excerpts from the original image, and from interpolated after 13 iterations ones are shown. The excerpts contain areas of strongly disturbed irregular grid. As can be seen, the interpolated image for fixed filter exhibits the same type of errors as filters from [4], black spots on borders between near and far objects, while the image processed by the space-variable filter is almost error-free. Moreover, details lost under black spots in the former image are somehow reconstructed in the latter one. There is a small window detail on the right side of the image that is better reproduced by the fixed filter, nevertheless, the overall performance improvement due to space-variable method is clearly visible.

4. CONCLUSION

We have presented the space-variable implementation of interpolating regularly sampled images from irregular grids based on POCS methodology. The new technique gives much better results in terms of PSNR, convergence rate, and visual quality than approaches in which bandwidth limitation operator is fixed (not space-variable). The simplest realization of such bandwidth limitation operator has been described, being a filter with two sets of coefficients, one used on well-defined parts of the irregular grid, and the other for processing sparcely sampled regions. The implementation is time efficient, but requiring a lot of computer memory. It is then interesting how this approach will work when applied to sophisticated, but time and memory efficient frequency-domain technique from [4].

5. REFERENCES

[1] R.D. Sauer, J.P. Allebach, 'Iterative reconstruction of band-limited images from nonuniformly spaced samples,' IEEE Trans. Circuits Syst., vol. 34, no. 12, pp. 1497-1506, 1987.

[2] H. Feichtinger, K. Grchenig, 'Theory and practice of irregular sampling,' in: Wavelet: Mathematics and Applications, eds.: Benedetto, J., Frazier, M., chapter 8, Boca Raton FL: CRC Press, pp. 305-363, 1994.

[3] A. Sharaf, F. Marvasti, 'Motion compensation using spatial transformations with forward mapping,' Signal Processing, Image Commun., vol. 14, pp. 209-227, 1999.

[4] R. Stasiski, J. Konrad, 'POCS reconstruction of stereoscopic views,' Signal Processing: Image Communication, accepted for publication, Oct. 2002, preliminary text in Proc. EUROIMAGE'01, Mykonos, Greece, pp. 41-44, 2001.

[5] R. Stasiski, J. Konrad, 'Improved POCS-based Image Reconstruction from Irregularly-spaced Samples', EUSIPCO-2002, Tulouse, vol. II, pp. 461-464, 2002.

[6] E. Dubois, 'The sampling and reconstruction of time-varying imagery with application in video systems,' Proc. IEEE, vol. 73, no. 4, pp. 502-522, Apr. 1985.

[7] P. Combettes, "The foundations of set-theoretic estimation," Proc IEEE, vol. 81, no. 2, pp. 182-208, 1993.

[8] R. Stasiski, J. Konrad, "POCS-based Image Reconstruction from Irregularly-spaced Samples", ICIP-2000, Vancouver, vol. II, pp. 315-318, 2000.

Figure 4: 60 × 180-pixel excerpts from original *Flowerpot* image (center), and its interpolations: space-variable (top), and fixed filter (bottom).